Theoretical study on strain-controllable gradient Schottky barrier of dumbbell-shape graphene nanoribbon for highly sensitive strain sensors

Qinqiang Zhang, Ken Suzuki, and Hideo Miura
Fracture and Reliability Research Institute, Tohoku University, Sendai, Miyagi, Japan
Tel: +81-22-795-4830, Fax: +81-22-795-4311, e-mail: kn@rift.mech.tohoku.ac.jp

Abstract **— The strain-induced change of electronic conduction properties in the dumbbell-shape graphene nanoribbon structure and the electronic band structure around the jointed interface between the metallic GNR (Graphene NanoRibbon) and the semiconductive GNR in the proposed dumbbell-shape structure were analyzed by using first-principles calculations in this study. The dumbbell-shape GNR exhibited a complicated current-voltage characteristics under the application of uniaxial strain. The main reason for the complicated behavior was attributed to the existence of the strain-induced change of gradient Schottky barrier around the newly formed atomic seamless interface between the metallic GNR and semiconductive GNR under the application of uniaxial tensile strain. The band diagram of the newly formed gradient Schottky barrier around atomic seamless interface was completely different with that of the conventional step-like metal-semiconductor interface. This energy height of gradient Schottky barrier can be modulated by applying an appropriate range of tensile strain. This strain-induced change of the electronic band structure of dumbbell-shape GNR showed a great potential for developing a highly sensitive strain sensor with stable electronic performance.**

Keywords — graphene nanoribbon, dumbbell-shape, strain-controlled, atomic seamless interface, first-principles

Introduction

Mobile health monitoring sensors with large deformability and sensitivity are indispensable for our sustainable and reliable life in an aging society with declining birthrate. Various types of sensors such as point of care devices for remote diagnostics, biochemical sensors for environmental monitors, light-sensitive sensors for ultraviolet rays' protection, and so on are eagerly to be developed and applied in our daily life. For instance, monitoring of slight change of blood pressure is necessary and it is well-known that there are strain-induced changes of various physical and chemical properties of materials. The stress and strain field in the required sensors is, therefore, necessary to be monitored to ensure the regular operation with high sensitivity and low cost. Thus, there is an enormous demand for highly sensitive strain sensors.

Recently, graphene-based strain sensors with high sensitivity and large deformability have been developed [1-3]. Graphene is a monolayer of graphite possessing a honey-comb-like unit cell of carbon atoms. In general, graphene sheets are good conductors, however, when graphene is cut into narrow ribbons with nanoscale widths, called graphene nanoribbons (GNRs), GNRs starts to exhibit semiconductive properties. GNRs are classified into two groups according to the structure of their ribbon edge: armchair GNRs (AGNRs) and zigzag GNRs (ZGNRs) [4]. ZGNRs possess a local electron orbital distribution around the zigzag edge due to the quantum confinement effect and exhibit metallic electronic properties regardless of the ribbon width. Furthermore, ZGNRs are not sensitive to the uniaxial strain [5]. On the other hand, AGNRs have been theoretically studied to exhibit semiconductive or metallic properties depending on their ribbon width, in other words, the total number of carbon atoms in the width direction. It also exhibits significant strain sensitivity in electronic band structure and electron transport properties, in other words, the piezoresistive effect [6]. To employ a semiconducting GNR as the sensing element, a metal electrode must be attached to the GNR to form stable ohmic contact and conduct current through the GNR. However, there is a large bandgap mismatch between metal electrode and semiconductive GNR, resulting in a non-negligible Schottky barrier. Up to now, a stable process of forming ohmic contact with low contact resistance between metal electrode and piezoresistive GNR has not been established yet.

In order to develop a simple and versatile method to form ohmic contact between metal electrodes and a semiconductive GNR, a novel structure, named as dumbbell-shape GNR structure has been proposed in our previous studies [7]. The schematic image of the dumbbell-shape GNR is shown in Fig. 1. The dumbbell-shape structure consists of one narrow segment sandwiched by two wide segments. The wide segments at both ends are metallic GNRs and they should be ensured to exhibit ohmic contact with metallic interconnections. The narrow segment is a semiconductive GNR which exhibits the periodic change between semiconductive and metallic properties as a strong function of strain. When the wide segment which show metallic properties is jointed with a semiconductive GNR, Schottky barrier should appear around the jointed interface. Since the metal-semiconductor junction at the interface of a DS-GNR is a completely atomically seamless single structure consisting only of carbon atoms, the junction interface is expected to have different characteristics from the conventional metal-semiconductor interface. In this study, the strain-induced change of electronic band structure and

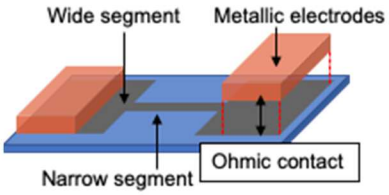

Figure 1: Schematic image of the dumbbell-shape graphene nanoribbon structure for a highly sensitive strain sensor

978-1-6654-0685-7/21/$31.00 ©2021 IEEE

electron transport properties in the proposed DS-GNR were investigated by using first-principles calculations based on density functional theory (DFT). The proposed DS-GNR structure exhibited a unique strain-induced change of gradient Schottky barrier behaviour between the metallic GNRs and piezoresistive GNRs. In addition, the height of Schottky barrier can be minimized by applying an appropriate range of strain.

Simulation model

The simulation model of the DS-GNR which consists of wide and narrow GNRs is shown in Fig. 2. In this study, four structural factors of the DS-GNR were defined: the width of the wide segment (W_W), the width of the narrow segment (W_N), the length of the narrow segment (L_N), and the length of the wide segment (L_W). The width was defined by the total number of carbon atoms connected as a dimer line along Y axis (width direction). The length, on the other hand, was defined as the number of units in a group of six-membered rings along the Z-axis (length direction). The region is enclosed by the dashed box as shown in Fig. 2. For example, the structure shown in Fig. 2 is denoted by (W_W, W_N, L_N, L_W) = (29, 07, 10, 05) using these structural factors. The wide segments were defined to possess metallic-like properties to ensure DS-GNR to have ohmic contact with external metal interconnection. For high strain sensitivity by using DS-GNR, the narrow segment was selected to have semiconductive properties with large bandgap at its initial strain state (0%) [8]. In this study, the local density of states (LDOS) was evaluated for each region defined by the dashed box to investigate the local electronic properties from the interface between the wide and narrow segments. The forbidden energy bandgap between the energy of the highest valence band and that of the lowest conductance band in the plot of LDOS was defined as local effective bandgap. It was evaluated from the central region of the wide segment Wp to the central region of the narrow segment Np, where p is an integer. The dashed box near the interface is the first layer (W1 or N1), and the central regions of the wide and narrow segments are the fifth layer (W5 and N5), respectively.

All simulations were conducted by applying first-principles calculations based on the DFT as packaged in SIESTA [9]. The current-voltage characteristics of the DS-GNR structure was investigated by the post-processing calculation code, TranSIESTA. The simulation model has enough vacuum space (at least 10 Å on each edge side) to eschew the effect from the neighboring molecule in the calculation. And the generalized gradient approximation (GGA) in the Perdew-Burke-Ernzerhof (PBE) form was utilized. The k-point sampling was optimized as 1×1×11, at which 11 is long the periodic direction (Z axis). It was enough to acquire the accurate electronic band structure of DS-GNR in which the increase of the k-point number has no effect on the change of it. In this study, solely the first model without applied tensile strain was fully relaxed. The calculations of DS-GNR structure were the single-step method under tensile strain to clarify the electronic band structure and transport properties in the definite strained states.

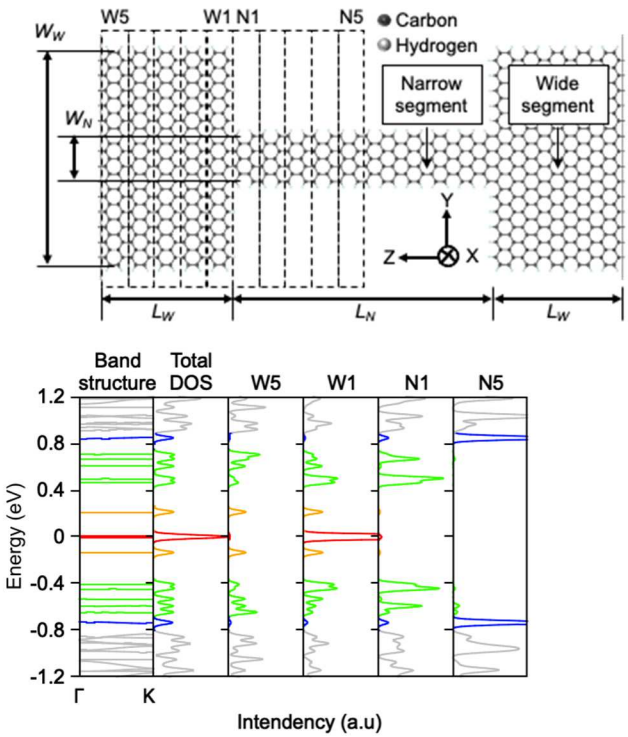

Figure 3: Electronic band structure and total density of states of (29, 07, 10, 05) DS-GNR, and its local density of states in the center region of wide segment (W5), in the interface region of wide segment (W1), in the interface region of narrow segment (N1), and in the center region of narrow segment (N5)

Localized electronic properties around the interface

At first, the band structure, total density of states (DOS), and local density of states (LDOS) in each region along the length direction of (29071005) DS-GNR are shown in Fig. 3. The different colors in the diagrams indicate electronic states with different energy levels near the Fermi level (0 eV). In the plot of the electronic band structure and total DOS, all 5 colors are contained. Gray-line energy states have deep energy states which are as reference in the figures. The concentration of the DOS was confirmed at the Fermi level in the W1 region around the jointed interface as indicated by red line. The intensity of the peak decreased from W1 to W5. Figure 4(a) shows the molecular orbital distribution with the highest energy in the valence band. Red color distribution has the corresponding energy levels with LDOS. It was confirmed that the concentrated DOS at the Fermi level was attributed to the electronic state localized at the zigzag edge. There were energy states continuously from W5 to the jointed region of the narrow segment (N1) as indicated by green lines. The intensity of these peaks decreased as the distance increased from the junction interface, and it disappeared in the N5 region. LDOS in N5 region is analogous to that of in single 7-AGNR. Figure 4(b) shows the molecular orbital distribution

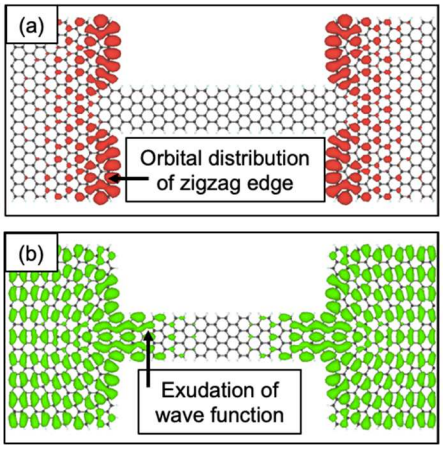

Figure 4: Spatial distribution of molecular orbitals around (a) Fermi level and around (b) energy states of -0.4 eV

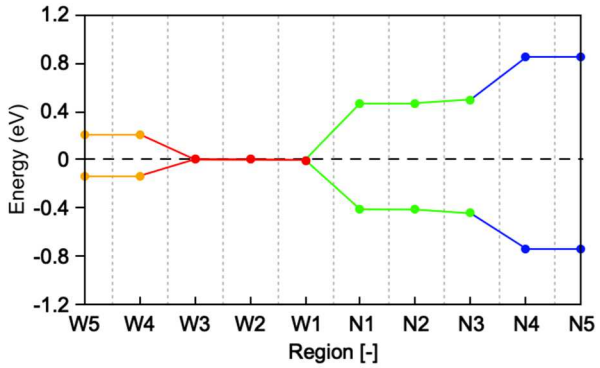

Figure 5: Energy states in lowest conduction band and highest valence band of (29, 07,10, 05) DS-GNR from the center region of wide segment (W5) to the center region of narrow segment (N5)

around the energy of -0.4 eV. The energy levels did not exist in the single 7-AGNR, but the distribution was found in the narrow segment. This distribution was formed by the exudation of a wave function from the wide segment into the narrow segment. As a result, the effective bandgap of the narrow segment monotonically decreased from the center region (N5) to the jointed interface region (N1).

Figure 5 shows the summarized sketch of the energy states based on the energy of the highest valence band and that of the lowest conduction band of DS-GNR. The color lines and points correspond to the energy states in Fig. 3. The energy barrier for electronic conduction between each region was defined by the energy difference of the lowest conduction band in each region. A clear energy difference in conduction band was observed between the junction interfaces, W1 and N1, indicating the existence of a large energy barrier (Schottky barrier) near the junction interface between the wide and narrow segments. In the narrow segment, the energy barrier increased from the interface region to the center region of DS-GNR. Due to the exudation of a wave function from the wide segment, the energy barrier of the narrow segment was not constant, and a graded Schottky barrier was found to distribute.

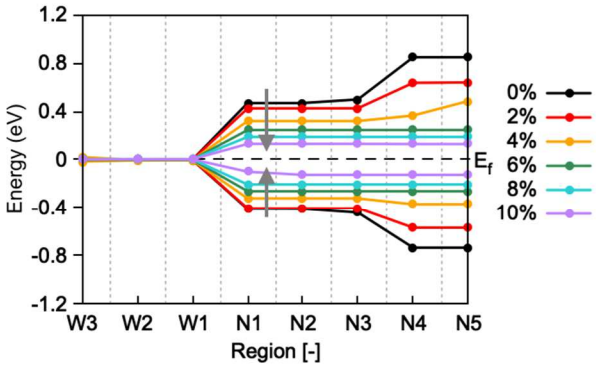

Figure 6: Strain-induced change of the energy states in the lowest conduction band and the highest valence band of (29, 07, 10, 05) DS-GNR from the center region of wide segment (W5) to the center region of narrow segment (N5) under uniaxial tensile strain from 0% (black line) to 10% (purple line)

Strain-induced change of the localized electronic properties

Figure 6 shows the summarized sketch of the energy states based on the highest valence band and the lowest conduction band of DS-GNR under uniaxial strain from 0% to 10%. The Fermi level E_f is at 0 eV as indicated by dashed line. The color lines from black to purple indicate energy states of valence band and conduction band under tensile strain from 0% to 10%, respectively. Based on the results of the energy states of valence band and conduction band from the center region of the wide segment to the center region of the narrow segment, the gradient Schottky barrier was clearly formed around the atomic seamless interface as indicated by black line. The energy barrier between the conduction band and the Fermi level was decreased with increase of strain as emphasized by gray arrows. When the magnitude of the applied strain was around 10%, the energy barrier between the conduction band and the Fermi level became small. The strain-induced change of effective bandgap was confirmed in the narrow segment which was analogous to that in the single 7-AGNR. In addition, the strain-induced change of the gradient Schottky barrier was observed. For the dynamic properties under strain, the large gradient Schottky barrier showed a negative effect because it affected the stability of the electron transport properties of DS-GNR. However, the Schottky barrier around the atomic seamless interface of DS-GNR was minimized by applying an appropriate strain. In addition, the piezoresistive effect was observed in the narrow segment of DS-GNRs due to the unique electronic properties of single GNRs. Therefore, DS-GNR has a great potential for the use in the next-generation strain sensors with stable electronic performance and high piezoresistive sensitivity.

Strain-induced change of electronic transport properties

I-V characteristics of DS-GNR structure (W_W, W_N, L_N, L_W) = (29, 07, 10, 05) as the example was summarized in Fig. 7. Uniaxial strain was applied from 0% to 10% and the analyzed I-V curves are shown from the black line to the purple line, respectively. The gray arrow briefly indicates the direction of

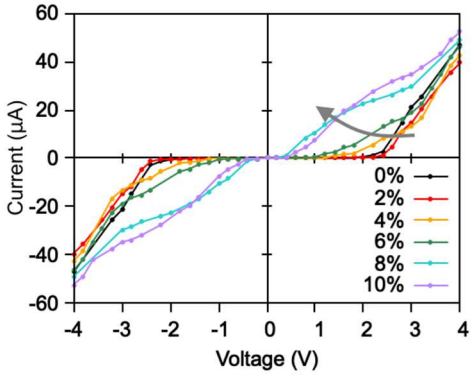

Figure 7: Strain-induced change of the current-voltage characteristics of (29, 07, 10, 05) DS-GNR under uniaxial tensile strain from 0% (black line) to 10% (purple line)

the change of the I-V curve under uniaxial tensile strain. No significant change in the I-V curve was observed under the strain from 0% to 2%, implying that the strain sensitivity in this strain region was expected to be small. As shown in Fig. 6, since the energy barriers between the wide segment and narrow segment were almost the same at 0%-strain and 2%-strain, the voltage at which current started to flow in the narrow segment (threshold voltage) did not change, and as a result, the I-V characteristics were similar. From 2%-strain to 8%-strain, the Schottky barrier around the interface was decreased and its threshold voltage of the structure decreased monotonically with the applied tensile strain from 2% to 8% (from red line to blue line). In this specific range, the strain-induced change of the I-V characteristics agreed well with that of the single GNR (L_N = 7). Therefore, the behavior of high sensitivity of single GNR was retained by utilizing DS-GNR structure based on the piezoresistive effect of the single semiconductive GNR. In the region from 8% to 10%-strain, the I-V characteristics were analogous to that of metallic properties with a small threshold voltage and less curved line. By applying an appropriate range of strain, the Schottky barrier around the atomic seamless interface was minimized and the I-V characteristics of DS-GNR showed a metallic-like properties as was expected above.

Conclusions

To develop a structural health monitoring system with low cost and high sensitivity and reliability for our stable daily life, a dumbbell-shape GNR structure was proposed to form the stable ohmic contact between a semiconductive GNR and external metal interconnection for highly sensitive strain sensors. It was found that even though the gradient Schottky barrier was formed between a metallic GNR and a semiconductive GNR, it was varied by applying uniaxial strain. Therefore, by applying an appropriate range of strain, it is possible to control the gradient Schottky barrier which is newly formed around the atomic seamless interface in one single molecular consisting of only carbon atoms. In addition, the high strain sensitivity of the electronic band gap was retained in the center region of the narrow segment of the DS-GNR under the application of an appropriate strain. Thus, DS-GNR-base sensors exhibit a stable electronic transport performance with a high strain sensitivity which is close to single GNRs. This result shows a great potential of the application of the DS-GNR structure to versatile next-generation strain sensors for mobile health monitoring system.

Acknowledgment

This research activity has been supported partially by Japanese special coordination funds 266 for promoting science and technology, Japanese Grants-in-aid for Scientific Research, and Tohoku 267 University. This research was supported partly by JSPS KAKENHI Grant Number JP20H02022. The authors acknowledge Center for Computational Materials Science, Institute for Materials Research, Tohoku University for the use of MASAMUNE-IMR.

Reference

[1] Yang, M., Sasaki, S., Ohnishi, M., Suzuki, K., & Miura, H. (2016). Electronic properties and strain sensitivity of CVD-grown graphene with acetylene. *Japanese Journal of Applied Physics*, *55*(4S), 04EP05.

[2] Goundar, J. A., Kudo, T., Zhang, Q., Suzuki, K., & Miura, H. (2019, November). Strain and Photovoltaic Sensitivities of Dumbbell-Shape GNR-Base Sensors. In ASME International Mechanical Engineering Congress and Exposition (Vol. 59476, p. V010T12A016). American Society of Mechanical Engineers.

[3] Suzuki, K., Nakagawa, R., Zhang, Q., & Miura, H. (2021). Development of Highly Sensitive Strain Sensor Using Area-Arrayed Graphene Nanoribbons. Nanomaterials, 11(7), 1701.

[4] Son, Y. W., Cohen, M. L., & Louie, S. G. (2006). Energy gaps in graphene nanoribbons. Physical review letters, 97(21), 216803.

[5] Sun, L., Li, Q., Ren, H., Su, H., Shi, Q. W., & Yang, J. (2008). Strain effect on electronic structures of graphene nanoribbons: A first-principles study. The Journal of chemical physics, 129(7), 074704.

[6] Li, Y., Jiang, X., Liu, Z., & Liu, Z. (2010). Strain effects in graphene and graphene nanoribbons: the underlying mechanism. Nano Research, 3(8), 545-556.

[7] Zhang, Q., Kudo, T., Gounder, J., Chen, Y., Suzuki, K., & Miura, H. (2019, September). Theoretical Study of the Edge Effect of Dumbbellshape Graphene Nanoribbon with a Dual Electronic Properties by First-principle Calculations. In *2019 International Conference on Simulation of Semiconductor Processes and Devices (SISPAD)* (pp. 1-4). IEEE.

[8] Kudo, T., Zhang, Q., Suzuki, K., & Miura, H. (2019, November). First Principle Analysis of the Effect of Strain on Electronic Transport Properties of Dumbbell-Shape Graphene Nanoribbons. In ASME International Mechanical Engineering Congress and Exposition (Vol. 59476, p. V010T12A010). American Society of Mechanical Engineers.

[9] Soler, J. M., Artacho, E., Gale, J. D., García, A., Junquera, J., Ordejón, P., & Sánchez-Portal, D. (2002). The SIESTA method for ab initio order-N materials simulation. Journal of Physics: Condensed Matter, 14(11), 2745.